tial for the growth of the cells, but they are routinely added to the medium. The basal medium excluding casein hydrolyzate is designated P-medium. The inorganic sources of nitrogen tested were ammonium citrate, ammonium tartrate, or ammonium nitrate.

In the medium containing only minerals, sucrose, auxin, and kinetin, there was some growth of the isolated cells (from 0.6 mg to 6 mg). In a medium with casein hydrolyzate but no sugar, growth was better (0.6 mg to 27 mg). When both casein hydrolyzate and sugar were present, there was marked increase in growth (0.6 mg to 183.3 mg). Thus, besides sugar, an organic nitrogen source (casein hydrolyzate) is apparently a primary need for the growth of these isolated cells. Trials were made with individual amino acids (at concentrations contained in 400 mg of casein hydrolyzate). Only additions of glutamic acid, lysine, and proline gave some growth response. Increased concentrations of casein hydrolyzate (800 to 1600 mg/liter) did not improve the growth; 400 mg/liter appeared to be the optimum requirement. However, if the cells were supplied with a mixture of organic (casein hydrolyzate) and inorganic (NH_4^+) sources of nitrogen, there was significant increase in the growth (Table 1).

As the higher growth values were obtained, there was a decrease in the amount of chlorophyll in the tissue produced by the isolated mesophyll cells. This fact is comparable to findings of experiments with *Euglena*. When grown at fairly high temperature for several successive generations, such cells replicate faster than the chloroplasts, giving rise to successively paler cells. The mesophyll cells exhibited a higher chlorophyll content when grown in the basal medium containing added ammonium nitrate than they did in medium with added ammonium citrate or tartrate.

To obtain some idea about the metabolic potential of the cells, and eventually to achieve their autotrophic growth, we omitted casein hydrolyzate from the basal medium (P-medium) and replaced it by one of the ammonium salts (Table 2; Fig. 1, a–c). At concentrations of 2000 to 2400 mg/liter, growth was insignificant.

Among the nutrients of the P-medium is $NaNO_3$, and additional NH_4NO_3 in the medium increased the concentration of NO_3^- relative to that of NH_4^+. The lack of growth at a lower concentration of NH_4NO_3 in the presence of $NaNO_3$ in the P-medium could be due to the fact that the isolated mesophyll cells lack an efficient nitrate-reductase system and thus cannot reduce nitrate to ammonia. Therefore, the presence of increased NO_3^- may in some way check the availability of NH_4^+ which could be absorbed by the cells. As soon as certain balance between NH_4^+ and NO_3^- is attained in the medium, NH_4^+ becomes available to the cells. In addition, the *p*H of the medium favors the uptake of NH_4^+ over that of NO_3^-. According to Arrington and Shive (*10*), a low *p*H favors nitrate uptake, and a high *p*H favors ammonia uptake. However, we made no such experiments with isolated mesophyll cells.

In the absence of $NaNO_3$ from the P-medium, the addition of NH_4NO_3 resulted in an increased growth (Table 3). The growth increased as the amount of ammonium nitrate added to the medium was increased; maximum growth was attained at 1600 mg/liter (Fig. 1d).

Thus, the isolated mesophyll cells can synthesize their own metabolites from the mineral nutrients. Ammonia seems to be one of the crucial requirements. For these cells, the only requirements for growth (by division and enlargement) are the minerals with an appropriate ammonia source, and energy source (sugar), auxin, and kinetin. The tissue mass produced by the isolated mesophyll cells in such a medium in shake cultures, when transferred to agar medium (*11*) supplemented either with ammonium citrate or tartrate, could grow continuously if subcultured at regular intervals.

P. C. Joshi
G. R. Noggle

Department of Botany,
North Carolina State University,
Raleigh 27607

References and Notes

1. E. Ball and P. C. Joshi, *Bot. Gaz.* **126**, 233 (1965).
2. E. D. Earle and J. G. Torrey, *Plant Physiol.* **40**, 520 (1965).
3. F. C. Steward, M. O. Mapes, A. E. Kent, R. D. Holsten, *Science* **143**, 20 (1964).
4. J. Bonner, in *Plant Biochemistry*, J. Bonner and J. E. Varner, Eds. (Academic Press, New York, 1965), pp. 862–863.
5. W. Halperin, *Science* **153**, 1287 (1966).
6. G. Haberlandt, *Sitzungber. Akad. Wiss. Wien., Abt.* **111**, 69 (1902).
7. P. C. Joshi and E. Ball, *Dev. Biol.*, in press.
8. E. Ball and P. C. Joshi, *Nature* **207**, 213 (1965).
9. D. I. Arnon, *Plant Physiol.* **24**, **1** (1949).
10. L. Arrington and J. Shive, *Soil Sci.* **39**, 431 (1935).
11. T. Murashige and F. Skoog, *Physiol. Plant.* **15**, 473 (1962).
12. We appreciate the cooperation of Drs. E. Ball and J. Kahn for providing us with their laboratory facilities. We also thank Dr. W. C. Gregory for help in many ways. Supported by NSF grant GB 3380.

25 October 1967

Comparative X-Ray and Neutron Diffraction Study of Bonding Effects in s-Triazine

Abstract. *X-ray and neutron-diffraction data were combined for study of deviations from spherical symmetry of the atomic charge distributions in the small organic molecule* s-*triazine. The results indicate that density has migrated from the atomic regions into the bonds and into the nitrogen lone-pair region. Refinement procedures for x-ray data, which do not take these bonding effects into account, give parameters containing small but measurable errors.*

In conventional refinement of x-ray data by least-squares techniques, all atoms are assumed to have spherical symmetry. In reality many atoms in molecules are in an asymmetric environment. Thus the centroid of the atomic charge density often does not coincide with the atomic nucleus, because of the presence of overlap density in the bond regions and lone-pair density in certain nonbonding regions (*1*). Atomic positions, as determined by x-rays, may therefore differ slightly from positions determined by neutron diffraction, which correspond to the locations of the atomic nuclei. Similarly, anisotropic x-ray temperature parameters may contain small contributions resulting from the diffuseness of the valence electron cloud due to bonding, rather than from genuine thermal motion.

I undertook to investigate these effects. The molecule of *s*-triazine was selected because (i) it is a simple molecule containing only first-row atoms, so that bonding effects are relatively important; (ii) it contains lone electron pairs on the nitrogen, aromatic C–N bonds, and C–H bonds, all of which are features of interest; (iii) as shown by Wheatley (*2*), the planar molecule occupies a highly symmetric position in the crystal, its center coinciding with the threefold axis of space group $R\bar{3}c$ (a, 9.647 Å; c, 7.281 Å), while all the other atoms are situated on three two-fold axes perpendicular to the threefold axis. The geometry of the molecule in the crystal is therefore completely described by three parameters: the distances of the C, N, H atoms from the threefold axis which are denoted by x_C, x_N, and x_H, below. The tensors describing the anisotropic thermal motions of the atoms are similarly restricted by symmetry and have four rather than six independent elements.

X-ray and neutron-diffraction data were collected at 24° to 26°C on the Brookhaven computer-controlled diffractometer system. The rhombohedral reciprocal lattice is highly symmetric. Each reflection was measured at least four times at different angular settings, and symmetry-equivalent sets were averaged after correction for absorption (*3*). Both Cu$K\alpha$ and Mo$K\alpha$ radiation were employed in the x-ray measurements (Table 1).

Both x-ray and neutron data were refined by least squares, with Wheatley's coordinates as starting parameters. The spherically symmetric form factors of Hanson *et al.* for C and N and of Stewart *et al.* for H (*4*) were used in refinement of the x-ray data. Results appear in Tables 2 and 3. The shifts in the positions of the atoms are small, except for the hydrogen atom (last two columns of Table 2), but all shifts are in directions predicted by theoretical calculations (*5*). Thus the x-ray nitrogen atom shows a small displacement toward the lone-pair region, while the x-ray carbon is displaced toward the center of the ring—in the direction of the bonding electrons of the two C–N bonds.

In addition, the x-ray temperature factors are generally larger than the corresponding neutron parameters; the fact that this effect is especially pronounced in the case of the carbon U_{22} indicates that the x-ray carbon atoms undergo an apparent thermal motion in the direction of the overlap density of the C–N bonds. For the nitrogen atom this effect is more than offset by the presence of the lone-pair density at the

Table 1. Diffraction data.

Item	Data		
	Neutron	X-ray	
		Cu	Mo
$(\sin\theta/\lambda)_{\max}$	0.66	0.51	1.0
Observed reflections, No.	83	68	94
Unobserved reflections, No.	43	7	457
Absorption correction, range	0.854–0.874	0.829–0.882	0.976–0.984

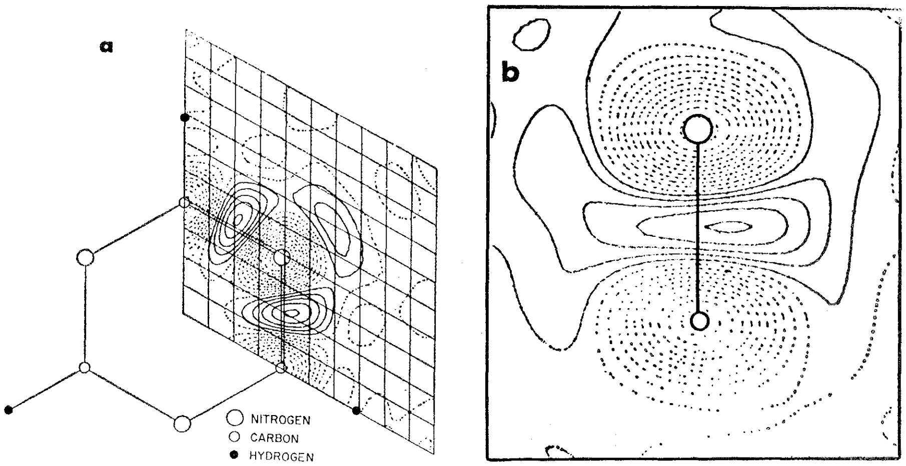

Fig. 1. (a) Section at $z = 0.25$ through molecular plane of the function $\Delta\rho_{X-N}$. This function is defined as $\sum_h \sum_k \sum_l F_X \cos 2\pi\,(hx + ky + lz) - \sum_h \sum_k \sum_l F_N \cos 2\pi\,(hx + ky + lz)$, in which F_X are the observed x-ray structure factors with the appropriate signs, and F_N are the corresponding structure factors calculated with neutron parameters and x-ray form factors. Contours at 0.05 eÅ^{-3}; zero contour and negative contours dotted. (b) Section through the C–N bond, perpendicular to the molecular plane; contours as in (a). Note that the extension of the bond peak in this section is compatible with π-bonding in the aromatic ring.

Table 2. Results of refinement. "Combined": Mo$K\alpha$ data plus weak reflections as measured with Cu$K\alpha$ radiation. Δ: Positive, away from center of ring; negative, toward center of ring. $\sigma(\Delta) = [\sigma^2(x_{\text{neutrons}} + \sigma^2(x_{\text{x-rays}})]^{\frac{1}{2}}$.

Item	Neutrons	X-rays			$\Delta = x_{\text{x-rays}} - x_{\text{neutrons}}$		$\Delta/\sigma(\Delta)$
		Cu	Mo	Combined	Fractions	(Å)	
Agreement factors (%)							
$R = \dfrac{\sum \big\lvert \lvert kF_0 \rvert - \lvert F_c \rvert \big\rvert}{\sum kF_0}$	7.3	5.4	4.5	5.0			
$R_w = \dfrac{\sum w \left\{ \big\lvert \lvert kF_0 \rvert - \lvert F_c \rvert \big\rvert \right\}}{\sum w \lvert kF_0 \rvert}$	5.3	5.5	3.7	3.9			
Fractional coordinates							
x_N	− 0.1400 ± 0.0005	− 0.1406 ± 0.0002	− 0.1408 ± 0.0002	− 0.1409 ± 0.0003	+ 0.0009	+ 0.0087	+ 1.5
x_C	+ 0.1328 ± .0008	+ 0.1316 ± .0004	+ 0.1317 ± .0004	+ 0.1313 ± .0004	− 0.0015	− 0.0145	− 1.8
x_H	+ .2411 ± .0014	+ .2284 ± .0045	+ .2334 ± .0054	+ .2286 ± .0043	− .0125	− .12	− 2.8

Table 3. Results of refinement. The U_{ij} are the coefficients in the expression $\exp[-(U_{11}h^2a^{*2} + U_{22}k^2b^{*2} + U_{33}l^2c^{*2} + 2U_{12}a^*b^*hk + 2U_{13}a^*c^*hl + 2U_{23}b^*c^*kl)]$, which multiplies the atomic scattering factor.

U	Temperature parameters U_{ij} (Å^2)				
	Neutrons	X-rays			$\Delta/\sigma(\Delta)$
		Cu	Mo	Combined	
		Nitrogen			
U_{11}	0.049 ± 0.002	0.056 ± 0.002	0.058 ± 0.002	0.055 ± 0.002	+ 2.1
U_{22}	.055 + .003	.056 ± .002	.051 ± .002	.052 ± .002	− 0.9
U_{33}	.115 ± .004	.129 ± .003	.134 ± .003	.133 ± .003	+ 3.6
U_{13}	−0.003 ± .004	−0.003 ± .002	.001 ± .004	−0.004 ± .002	− 0.2
		Carbon			
U_{11}	0.052 ± 0.003	0.054 ± 0.002	0.052 ± 0.002	0.053 ± 0.002	+ 0.2
U_{22}	.052 ± .004	.076 ± .002	.079 ± .003	.078 ± .003	+ 5.2
U_{33}	.105 ± .006	.113 ± .003	.108 ± .003	.109 ± .003	+ 0.6
U_{13}	.002 ± .005	.004 ± .002	−0.003 ± .005	.002 ± .002	0
		Hydrogen			
U_{11}	0.070 ± 0.008	0.075 ± 0.021	0.067 ± 0.018	0.068 ± 0.018	
U_{22}	.075 ± .008	.055 ± .026	.045 ± .024	.032 ± .022	
U_{33}	.199 ± .015	.173 ± .043	.187 ± .042	.167 ± .037	
U_{13}	−0.004 ± .008	−0.002 ± .021	.049 ± .021	.050 ± .018	

"other side" of the atom. These effects are pictured in Fig. 1, which was obtained by subtracting from the electron density, as derived from the x-ray observations, the density calculated with the neutron parameters and spherically symmetric x-ray scattering factors. Relatively large peaks are found in the section through the molecular plane at $z = 0.25$, which is the one reproduced in Fig. 1.

In particular, density is seen to have migrated from the atoms into the bonding region between the carbon and nitrogen atoms, and into the lone-pair region of the nitrogen atom; on the other hand, only a small maximum is observed in the region of the C–H bond. Integration of the electron density, according to a method developed by Coppens and Hamilton (*6*), shows that 0.08 electron is contained in a box, centered at the midpoint of the C–N bond and measuring 0.47 by 1.0 by 1.45 Å, parallel to the bond, perpendicular to the bond in the plane of the molecule, and perpendicular to the plane of the molecule, respectively. One should note that the nitrogen lone-pair peak would be lower or absent, and the C–N bond peaks would be higher, if a prepared-state nitrogen atom, rather than a spherically symmetric atom, had been substracted from the x-ray density.

Quantitative comparison with theoretical difference-density maps is possible; such comparison would, however, be more meaningful if the thermal motion in the crystals were suppressed by collection of the data at lower temperatures. Such collection would (i) provide more-accurate neutron parameters, (ii) reduce anharmonicity effects which are not allowed-for in the thermal-motion treatment of the data, and (iii) reduce the history of thermal motion to be superimposed on theoretical maps before the comparison can be made. Unfortunately *s*-triazine was found to undergo a phase transition on cooling at about −40°C, but low-temperature work on other, similar, molecules is now in progress.

For detailed analyses of charge distributions one should determine the positional and temperature parameters from neutron-diffraction data only. The x-ray least-squares refinement can then be based on the occupancy factors of localized molecular orbitals, orbital exponents, and similar parameters. A need exists for suitable algorithms for such a treatment that will permit direct comparison with the corresponding theoretical values.

P. COPPENS

Department of Chemistry, Brookhaven National Laboratory, Upton, Long Island, New York 11973

References and Notes

1. P. Coppens and C. A. Coulson, *Acta Cryst.* **23**, 18 (1967); B. Dawson, *ibid.* **17**, 990 (1964); R. Mason and G. B. Robertson, in *Advances in Structure Research by Diffraction Methods*, R. Brill and R. Mason, Eds. (Vieweg-Interscience, Braunschweig-New York, 1966), vol. 2, p. 53.
2. P. Wheatley, *Acta Cryst.* **8**, 224 (1955).
3. P. Coppens, L. Leiserowitz, D. Rabinovich, *ibid.* **18**, 1035 (1965).
4. H. P. Hanson, T. Herman, J. D. Lea, S. Skillman, *Acta Cryst.* **17**, 1040 (1964); R. F. Stewart, E. R. Davidson, W. T. Simpson, *J. Chem. Phys.* **42**, 3175 (1965).
5. P. Coppens, unpublished.
6. ——— and W. C. Hamilton, *Acta Cryst.*, in press.
7. I thank A. L. Bednowitz for assistance in collecting the x-ray data on the automatic diffractometer system.

7 August 1967

Gibberellin Delays Ripening of Tomatoes

Abstract. *Treatment with gibberellic acid, at concentrations as low as* 10^{-7}M, *of intact tomato fruits, or of pieces in tissue culture, markedly retarded ripening in terms of development of redness. Ethylene stimulations of color development were prevented by treatment with gibberellic acid, but ethylene stimulations of respiration were not. Gibberellin can delay the progress of some components of the ripening of fruit, preventing some of the changes triggered by ethylene.*

In many fleshy fruits, ripening is probably regulated by the production of ethylene, which then triggers a dramatic respiratory rise (*1*); yet there is evidence of the existence in fruits, especially in those remaining on the plant, of factors that defer readiness for ripening (*2*). In tomato fruits, ripening can be deferred by application of inhibitors such as dinitrophenol (*3*). Recent reports that application of gibberellin could cause regreening in citrus fruits (*4*) suggested the possibility that gibberellins may defer ripening. This possibility was especially appealing in view of the reports of declines in content of natural gibberellin in fruits during maturation (*5*).

The dipping of mature green fruits of tomato (*Lyspersicon esculentum* L. var. Ailsa Craig) into solution of gib-

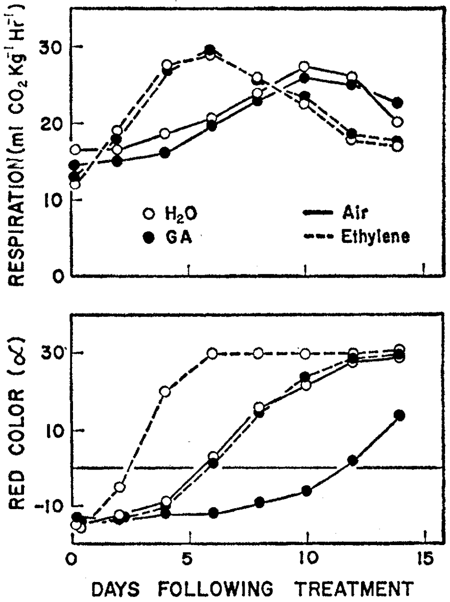

Fig. 1. Ripening of intact tomato fruits, as modified by treatments with gibberellin and ethylene: data for respiration (top) and for development of redness (bottom). *GA*, gibberellic acid.